We are IntechOpen, the world's leading publisher of Open Access books Built by scientists, for scientists

4,800
Open access books available

122,000
International authors and editors

135M
Downloads

Our authors are among the

154
Countries delivered to

TOP 1%
most cited scientists

12.2%
Contributors from top 500 universities

CLARIVATE ANALYTICS BOOK CITATION INDEX INDEXED

WEB OF SCIENCE™

Selection of our books indexed in the Book Citation Index in Web of Science™ Core Collection (BKCI)

Interested in publishing with us?
Contact book.department@intechopen.com

Numbers displayed above are based on latest data collected.
For more information visit www.intechopen.com

8

Earthquake Response Analysis and Evaluation for Earth-Rock Dams

Zhenzhong Shen, Lei Gan, Juan Cui and Liqun Xu
State Key Laboratory of Hydrology-Water Resources and Hydraulic Engineering, Hohai University
China

1. Introduction

An earthquake is any shaking of the ground, usually intense shaking of the ground - caused by either natural sources or by humans. There are many different types of earthquakes. The most common is tectonic earthquake, which occur when rocks in the earth's crust break due to geological forces created by movement of tectonic plates. Another type of earthquake is called volcanic earthquake, occurring in conjunction with volcanic activity. And also there are various types of earthquakes caused by man-made activities, which caused directly by human involvement, has been recorded as a result of water filling large dams, development of mineral, geothermal and hydrocarbon resources, waste injection, underground nuclear explosions and large-scale construction projects. This type of earthquake includes collapse earthquake, explosion earthquake and induced earthquake due to water filling large dams (Talwani, 1997; Chen & Talwani, 1998) and so on. Earthquake is the rapid vibration of the earth surface whose acceleration motion can easily cause the destruction of hydraulic structures. The relative deformation of the hydraulic structures increases when the inertial force caused by the earthquake increases suddenly. For the hydrodynamic pressure acting on the reservoir, dam foundation may appear relative deformation or different stage deformation. For example, those parts of concrete dams, including dam crest, fold slope, orifice inside the dam and corridor, are easily cracked, which may damage and then cause the leakage of the dam body, even the collapse of the structures after the earthquake. As it to the earth-rock dam, it is easy to appear cracks in dam in the process of the earthquake, meanwhile, dam foundation or dam body may collapse caused by earthquake liquefaction if the sands inside them are not fully roller compaction. Thus earthquake may cause the unsafe of the hydraulic structures, even dam breach which may threatened the life and property safety of the people downstream the river.

On May 12, 2008, a magnitude destructive earthquake (M_s=8.0), with the epicenter in Wenchuan County, struck Sichuan province, in southwestern China, killing more than 100,000 people. The earthquake was the largest and most destructive to strike China since the 1976 Tangshan earthquake, which killed more than 240,000 people (Pei et al., 2010; Wang et al., 2010; Cao et al., 2011). On January 12, 2010, a massive 7.3-magnitude earthquake has struck the Caribbean nation of Haiti. The earthquake struck about 15km (10 miles) south-

west of Port-au-Prince which is the capital city of Haiti. Approximately 230,000 people died immediately or during ensuing weeks, mostly due to acute trauma (Kenneth, 2011). The most devastating earthquake (M_s=9.0) in Japan after the 1923 Great Kanto earthquake hit the eastern Japan in the afternoon of March 11, 2011. Nearly 30,000 people were killed or missed in the Tohoku earthquake and the ensuing monster tsunami (Takewaki et al., 2011). In this paper, the non-linear FEM is adopted to calculate the Wenchuan earthquake response. Then, the earthquake-resistance safety of the Bikou dam is evaluated.

1.1 Bikou earth core dam

The Bikou hydropower station is located on the Bailong River in Gansu province of China, where is about 240km away from the epicenter of Wenchuan earthquake, China, May 12, 2008(Chen et al., 2008; Yu et al., 2009; Lin et al., 2009). The Bikou earth core rockfill dam is a 100m graduate earth-rock dam (Gu, 1989). According to the earthquake loss survey and preliminary report of the Bikou hydropower project suffered "5.12" Wenchuan earthquake, some damage appeared inside Bikou dam, but no dam slope slide and instability damaged phenomenon happened after the earthquake (Zhou et al., 2009; Pan, 2009).The normal water level of the reservoir is 707.0m, and its relative reservoir capacity is 5.21×10^8 m^3. The dam is earth core rockfill dam with height of 101.8m, where the typical cross section of the dam is shown as in Fig.1. The ratio of the upstream slope of the dam are 1:1.8 and 1:2.3 respectively, and the downstream slope are 1:1.7, 1:1.85, 1:2.2 and 1:1.5 respectively. Its width of dam crest is 7.6 m at elevation 710.00m, and the crest length of dam is about 297.36 m. The dam is located in a roughly symmetric valley of V-type, the slope of river bank is about 50-60 degree, and the one of right bank is about 35-45 degree. The depth of overburden layer on the riverbed is about 25-34 m. The core wall in the riverbed area is built on the natural sandy gravel layer, the width of core wall crest is 4.0m at elevation 709.00-710.00m, and the ratio of the upstream slope of the core wall are 1:0.2 and 1:0.25 respectively, the section of the dam along the dam axis is shown as in Fig.2. Two concrete cut-off walls are adopted to connect the soil core wall and the bedrock. The first one built along the dam axis inserts the bedrock with the thickness 1.30m and crest the elevation 630.00m. And the second concrete one is located at the dam axis downstream 12m, inserting the bedrock with the thickness 0.80m and the crest 653.00m. The spillway buildings are made up of one spillway on the right bank, one desilting tunnel and two spillway tunnels in the left bank.

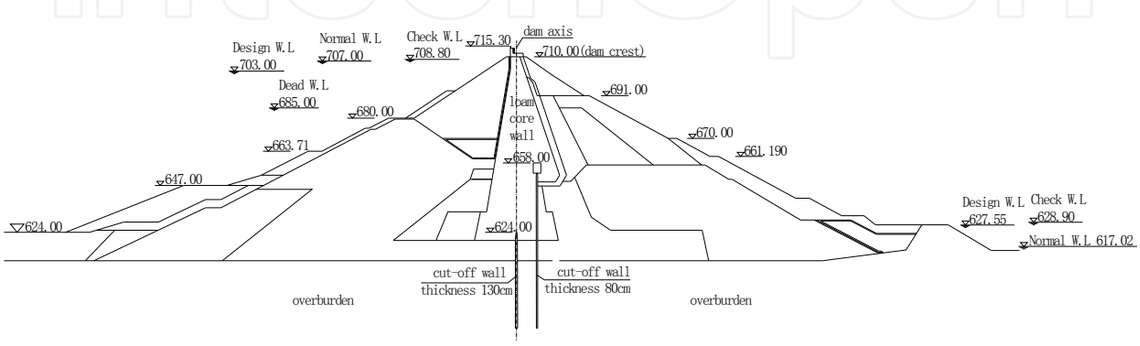

Fig. 1. Typical cross section of the dam

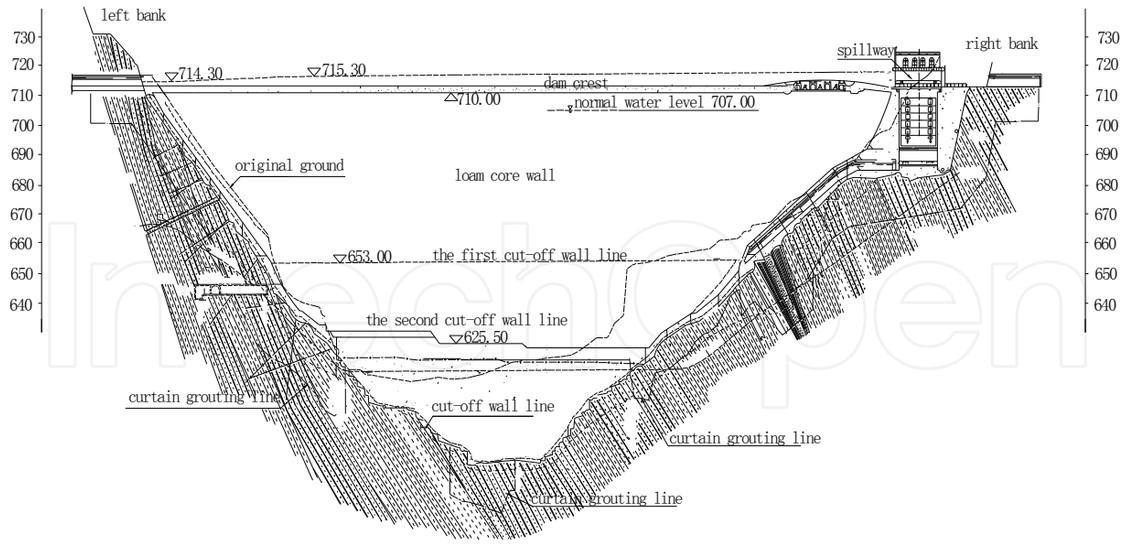

Fig. 2. Section of the dam along the dam axis

1.2 Geological conditions

In the dam site area, the fractures are developed, mainly are the bedding extrusion fracture zones and the slow obliquity faults. Most of the fractures are the tension and twist fractures of steep obliquity, and the slow obliquity fractures in the SN, NNE and EW directions. The faulted structures are mainly as follow: the fault F9, F1, F6 and F14, broken bandwidth 0.3 ~ 3.0m, mainly for fault mud and rock. The fracture zones are mainly made up of fault mud and rock, with width of 0.3-3.0m.

2. Calculation model

2.1 Static analysis model

2.1.1 Control equation of FEM

According to the displacement solution, the basic balance equation of the nonlinear finite element method is as follows

$$\left[K(u)\right]\{u\} = \{R\} \tag{1}$$

Where $\left[K(u)\right]$ is overall strength degree matrix, $\{u\}$ node displacement array and $\{R\}$ node load array.

This equation can be solved by the incremental early strain gauge method, where the basic balance equation holds:

$$[K]\{\Delta u\} = \{\Delta R\} + \{\Delta R_0\} \tag{2}$$

Here, $\{\Delta u\}$ is nodal displacement incremental array, $\{\Delta R\}$ node load incremental array and $\{\Delta R_0\}$ the equivalent node load array of initial strain.

2.1.2 Constitutive model

In the static analysis, the soil materials and overburden layer materials are regarded as elastic-plastic object, where the Duncan-Zhang's nonlinear-elastic (E-B) model (Duncan & Chang, 1970) is carried out. The concrete and bedrock are regarded as linear elastic objects, which obey the generalized Hook's law.

2.2 Dynamic analysis model

2.2.1 Control equation of FEM

The dynamic equilibrium equation can be described as follows after the calculation domain is discretized by the finite element method

$$[M]\{\ddot{\delta}\}+[C]\{\dot{\delta}\}+[K]\{\delta\}=\{F(t)\} \tag{3}$$

Here, $\delta,\dot{\delta},\ddot{\delta}$ are nodal displacement, nodal velocity and nodal acceleration respectively, $\{F(t)\}$ nodal dynamic loading, $[M]$ mass matrix, $[K]$ strength degree matrix, $[C]$ damping matrix obtained by $[C]=\lambda\omega[M]+\lambda[K]/\omega$, where ω is the first mode for vibration frequency and λ the damping ratio.

Eq.(3) can be gradually integral solved by the Wilson linear acceleration method (Wilson – θ method), which can instead by the following equations.

$$[\bar{K}]\{\delta\}_t=\{\bar{F}\}_t \tag{4}$$

$$[\bar{K}]=[K]+\frac{6[M]}{dt^2}+\frac{3[C]}{dt} \tag{5}$$

$$\{\bar{F}\}_t=\{F\}_t+[M]\{A\}_t+[C]\{B\}_t \tag{6}$$

$$\{A\}_t=\frac{6}{dt^2}\{\delta\}_{t-dt}+\frac{6}{dt}\{\dot{\delta}\}_{t-dt}+2\{\ddot{\delta}\}_{t-dt} \tag{7}$$

$$\{B\}_t=\frac{3}{dt}\{\delta\}_{t-dt}+2\{\dot{\delta}\}_{t-dt}+\frac{dt}{2}\{\ddot{\delta}\}_{t-dt} \tag{8}$$

$$\{\dot{\delta}\}_t=\frac{3}{dt}\{\delta\}_t-\{B\}_t \tag{9}$$

$$\{\ddot{\delta}\}_t=\frac{6}{dt^2}\{\delta\}_t-\{A\}_t \tag{10}$$

The iterative method is adopted with the consideration of the variations of dynamic shear modulus and damping ratio in calculation process after the average dynamic shear strain change. In the iteration process the convergence criterion is

$$\left|\frac{G^{i-1}-G^{i}}{G^{i}}\right|<0.1 \tag{11}$$

Here, G^{i} is the new shear modulus and G^{i-1} the last shear modulus. The maximum iteration times is taken for 6 to lest the iterative calculation into dead circulation.

2.2.2 Constitutive model

In the dynamic analysis (Mejia et al., 1981a, 1982b; Shen et al., 2006a, 2010b), the equivalent nonlinear viscoelastic model is applied in the dynamic calculation and analysis, the soil materials and the overburden layers are assumed to be viscoelastic bodies. They reflect nonlinearity and hysteretic nature of the dynamic stress-strain relation by using of the equivalent dynamic shear modulus G and equivalent damping ratio λ, which can be expressed as the function between the equivalent shear modulus and damping ratio and the dynamic shear strain amplitude. The key point of this model is to confirm the relationship between the maximum dynamic shear modulus $G_{\max}$ and the average effective stress σ_0'. In this paper, the Hardin-Drnevich model (Hardin & Denevich, 1972a, 1972b) is used, where the dynamic shear modulus and damping ratio can be calculated as follows

$$G=\frac{G_{\max}}{1+\gamma/\gamma_{\gamma}} \tag{12}$$

$$\lambda=\lambda_{\max}\frac{\gamma/\gamma_{\gamma}}{1+\gamma/\gamma_{\gamma}} \tag{13}$$

$$G_{\max}=K'p_a\left(\frac{\sigma_0'}{p_a}\right)^{n} \tag{14}$$

Where σ_0' is average effective stress, P_a atmospheric pressure, K' modulus coefficient and n is modulus exponent. Here, $G_{\max}$, σ_0' and p_a have the same dimension. The relation curves of dynamic shear strain γ to dynamic shear modulus and damping ratio can be obtained by dynamic tri-axial test (Xenaki & Athanasopoulos, 2008; Zegha & Abdel-Ghaffar, 2009). When having dynamic calculation, the related relation curve can be inputted directly, and then interpolate and extent the values according to the strain values for the calculation.

The dynamic model of contact face elements referred to the test results of Hohai University, China. The relationship between shear rigidity K and dynamic shear strain γ is described as follow

$$K=\frac{K_{\max}}{1+\frac{MK_{\max}}{\tau_f}\gamma} \tag{15}$$

The shear rigidity K and damping ratio λ have the following relationship:

$$\lambda = \left(1 + \frac{K}{K_{\max}}\right)\lambda_{\max} \tag{16}$$

$$K_{\max} = C\sigma_n^{0.7}\ ,\ \tau_f = \sigma_n \tan\delta \tag{17}$$

Where σ_n is the normal stress on contact face, δ the angle of internal friction on contact face, $\lambda_{\max}$ the maximum damping ratio and M , C are the test parameters.

2.3 Stability evaluation

The stress of element is used to calculate the factor of safety and evaluate its stability, thus the position of slide surface can be obtained. According to the Mohr-Coulomb criterion, the regions whose local safety factors are less than 1.0 are combined together to obtain the most dangerous multi-slip surface. The factor of safety on the surface is defined as the ratio of anti-sliding force to sliding force, and then the relationship between factors of safety and time can be obtained during the earthquake period. In this way, the anti-sliding stability is evaluated by stress when considering the unstable duration of earthquake.

During an earthquake, the dynamic strength of rockfill material is not always less than its static strength, at least we can assume it is equal to static strength. Taking compressive stress as positive and tensile stress as negative, after obtaining the static stress and dynamic stress under an earthquake by finite element method, the local factor of safety of an element can be calculated by the following formula

$$LF_s = \frac{2c\cos\varphi - (\sigma_1 + \sigma_3 - 2u_d)\sin\varphi}{\sigma_1 - \sigma_3} \tag{18}$$

Where c is cohesion, φ the angle of internal friction and σ_1 , σ_3 are the maximum and minimum principal stresses.

The u_d can be calculated by the formula as follow

$$u_d = \frac{(1+\mu)(\sigma_{1d} + \sigma_{3d})}{3} \tag{19}$$

Here, μ is Poisson's ratio and σ_{1d} , σ_{3d} are dynamic stresses respectively.

3. Working behavior of Bikou earth-rock dam

According to the actual engineering conditions of the Bikou earth core rockfill dam, the 3-D non-linear FEM static and dynamic models of the dam are set up to calculate and analyze the stress and deformation characteristics of dam, including the deformation and stress of the dam shell, core wall, two cut-off walls, overburden layers, bedrock and so on. In order to consider the construction process, the process of filling the dam is divided into 15 levels to simulate, and the reservoir impoundment process is divided into 3 levels.

3.1 Initial stress field of dam

In order to calculate the earthquake responses of dam, the initial stress field of dam must be determined firstly. Thus, the 3-D finite element model is created to simulate the construction process of dam and reservoir impounding, and the initial stress field of dam before earthquake can be obtained.

3.1.1 Finite element model

According to the actual situation of the Bikou dam, the 3-D finite element model of the dam and its foundation is set up, which has simulated the geometry and material partition of the dam and its foundation. The control section super-element finite element mesh automatic division technique is adopted to generate the information of finite element model, and furthermore the super-element can be encrypted to form finite element. Based on requirements of structural characteristics, stage loading and forming the super-element grid, a set of control sections with 19 sections horizontal are selected. Then the dam and its foundation are discretized, and the supper-element grid is built up. After the super-element gird is discretized further more, the super-element gird is created whose total nodes are 31523 and total element numbers are 30087. The finite element mesh of the dam and its foundation and its core wall are shown as in Fig.3.

Select domain of the calculation model. 1) The distance from the upstream boundary to the dam axis of the river bed section is about 363.40m (approximately 1.0 times of dam height). 2) The distance from the downstream boundary to the dam toe of the river bed section is around 401.00m. 3) The distance from the left boundary to the right boundary is about 698.18m (approximately 2.0 times of dam height). 4) The vertical distance from the bottom boundary to the dam foundation surface is about 241.80 m.

The coordinate system is set up as following. The X-axis is along stream from up to down with zero at dam axis, the Y-axis is along dam axis from right bank to left bank, and the Z-axis is vertical corresponding to the elevation.

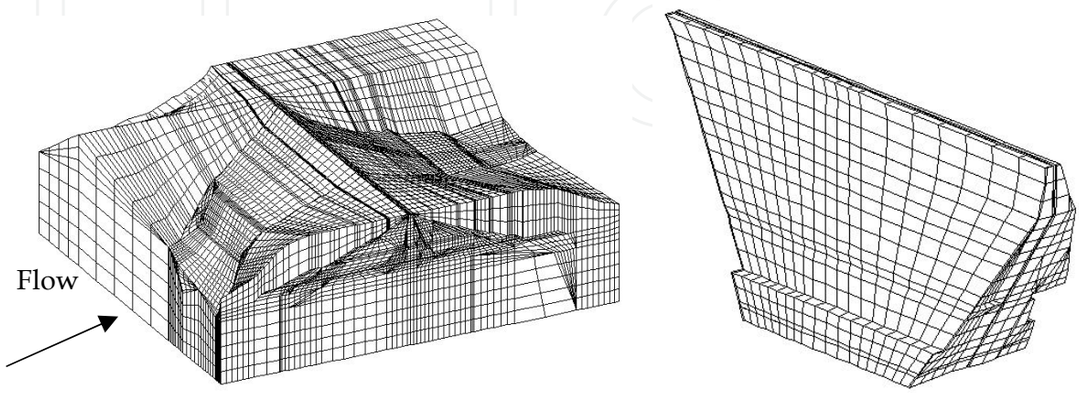

(a) dam body and foundation (b) core wall

Fig. 3. Finite element grid

3.1.2 Material parameters

The Duncan-Chang's nonlinear-elastic (E-B) model is carried out for the core wall and each district materials of the dam shell. According to indoor tests and engineering experience, the static material parameters of the dam are shown as in Table 1 and Table 2. And the parameters of the contact surface are shown as in Table 3.

Material types	$\gamma/kN\cdot m^{-3}$	E/kPa	ν
Concrete	24.5	1.8×10^{7}	0.20
Bedrock	26.0	1.0×10^{7}	0.25
Core wall settlings	24.0	8.0×10^{3}	0.35

Table 1. Parameters of linear elastic model

Material types		γ /kN·m^{-3}	c /kPa	K	n	R_f	K_b	m	$\Delta\varphi$ / ^{o}	K_{ur}	n_{ur}
core wall	W	20.7	100	190	0.42	0.81	120	0.86	2.1	450	0.30
	S	21.1	100	150	0.42	0.81	115	0.50	1.6	150	0.33
filter	W	22.1	0	750	0.40	0.75	460	0.80	4.8	600	0.33
	S	23.3	0	650	0.40	0.75	460	0.77	4.4	600	0.33
rockfill	W	21.2	0	1000	0.45	0.80	400	0.75	6.0	1500	0.33
	S	23.6	0	800	0.45	0.80	380	0.70	5.6	1500	0.35
ballast	W	21.4	0	600	0.45	0.80	350	0.69	4.1	860	0.30
	S	23.3	0	400	0.45	0.80	300	0.67	3.6	860	0.30
gravel (dam)	W	22.1	0	900	0.50	0.75	460	0.80	7.5	1700	0.25
	S	23.3	0	850	0.50	0.73	460	0.77	7.5	1700	0.23
gravel (mud)	W	22.5	0	500	0.45	0.74	300	0.79	3.3	900	0.30
	S	23.3	0	300	0.45	0.72	200	0.77	2.8	900	0.30
pebble	W	17.9	0	850	0.40	0.81	400	0.70	5.2	1300	0.33
	S	21.3	0	850	0.40	0.81	400	0.70	5.2	1300	0.33
gravel	S	23.9	0	700	0.50	0.70	320	0.78	7.6	1400	0.45

Table 2. Parameters of Duncan-Chang's model

Material	δ / ^{o}	K_s /×10^4	n_s	R_{fs}	C_s /kPa·m^{-3}
Loam /concrete	14.0	2.30	0.69	0.75	0
Sandy gravel / concrete	32.2	4.00	0.65	0.75	0
Loam /Loam	17.3	1.80	0.70	0.88	68
Bedrock /concrete	35.0	6.00	0.20	0.80	0
Bedrock /the settlings	30.0	3.00	0.70	0.80	0

Table 3. Parameters of contact surface

3.1.3 Displacement and stress field of dam

By use of the stage loading method to simulate the construction process of dam and reservoir impounding, the displacement field and stress field of dam under normal water level condition are obtained. Here, as examples, the displacement and stress distribution on the maximum transverse cross section of dam (Y=210m) and dam axis maximum longitudinal section of dam (X=-10m) are shown as in Fig.4 ~Fig.6.

Here, the displacement along the coordinate axis direction is positive, that is, the horizontal displacement along the flow with the direction of upstream point to the downstream is positive, the positive horizontal displacement along the dam axis direction is from the right bank to the left, and the positive vertical displacement is from bottom to up. The unit of the displacement is "mm" in some figures. The compressive stress is positive, and the tensile stress is negative. The unit of the stress is "kPa" in some figures.

1. Dam shell

Under normal water level condition, the maximum horizontal displacement pointing to the upstream and the downstream respectively is -289mm and 1132mm.The maximum value appears in the lower crust, close to the slope. The dam horizontal displacement distribution along the dam axis direction shows that the horizontal displacement value along dam axis direction is small. And the maximum settlement occurs in the upstream dam shell which is near the dam axis in the middle of the river. The maximum vertical displacement of the dam body is 1273mm, accounts for about 1.2% of the maximum height.

The maximum first principal stress of the dam body is 2534kPa, the maximum second principal stress is 2445kPa and the maximum third principal stress is 1842kPa. The maximum principal stress of the upstream and downstream dam shell occurs at the bottom of dam near the dam axis. The shear stress level of most rock-fill units are less than 0.85, no the shear failure zone appears in the dam body. It indicates that the dam is stable.

2. Core wall

The maximum horizontal displacement pointing to the downstream of the loam core wall is 812mm.The maximum horizontal displacements of core wall along dam axis direction is 181mm, pointing to the left bank. And the maximum vertical displacement of core wall is 1413mm, appearing in the upstream of the core wall near the dam axis where the elevation is 657.00m at the deepest valley section. The maximum first principal stress of the core wall is 1839kPa, the maximum second principal stress is 1373kPa, and the maximum third principal stress is 1256kPa.

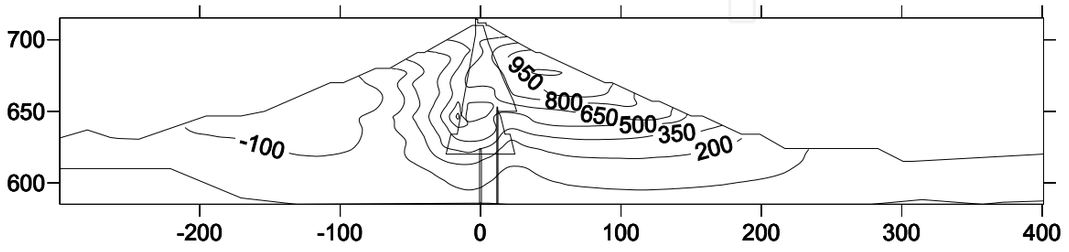

(a) X-displacement

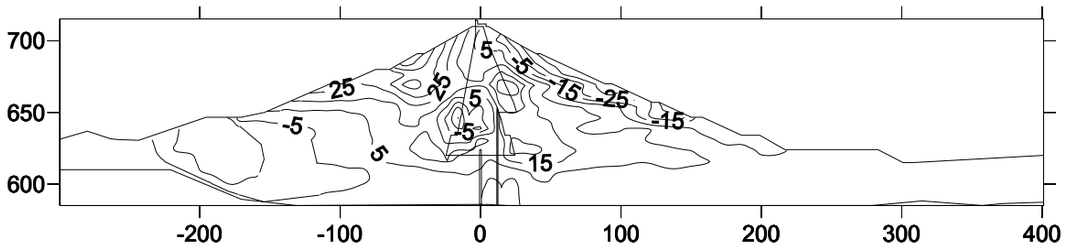

(b) Y-displacement

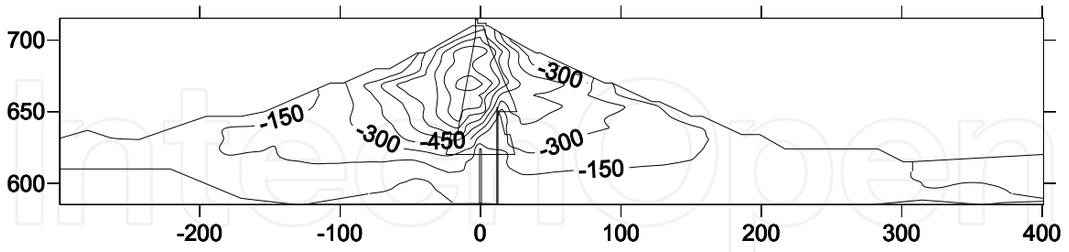

(c) Z-displacement

Fig. 4. Displacement distribution on section Y=210m (unit: mm)

Under normal water level condition, although core wall stress is smaller than depletion layer stress, but no tensile stress appeared, so the loam core wall won't produce pull crack. Meanwhile, for the strength and modulus of core wall is lower and the core wall is easy to adapt to deformation, core wall stress levels are lower. It indicates that the core wall is stable.

3. Cut-off wall

The maximum horizontal displacement of the first cut-off wall is 469mm, pointing to the downstream, and the vertical displacement is -112mm, and that of the second cut-off wall are 583mm and -129mm respectively. The maximum first principal stress of the first concrete cut-off wall is 9806kPa, the maximum third principal stress is 714kPa, and that of the second one are 16844kPa and 1094kPa respectively.

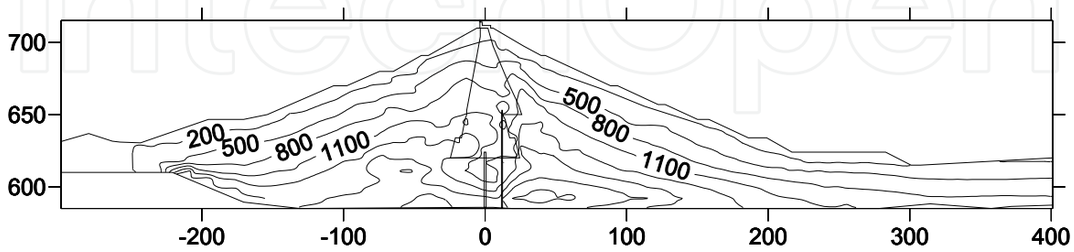

(a) the first principal stress (unit: kPa)

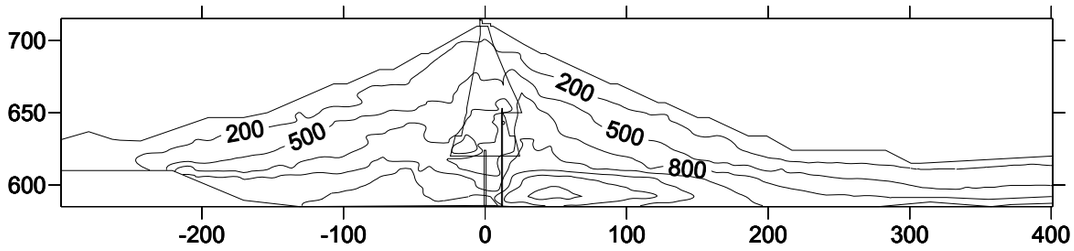

(b) the second principal stress (unit: kPa)

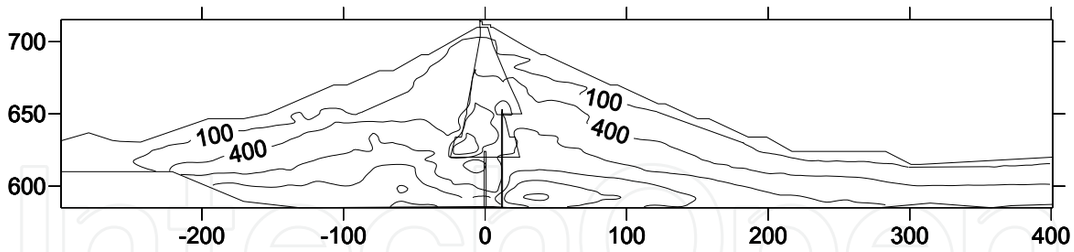

(c) the third principal stress (unit: kPa)

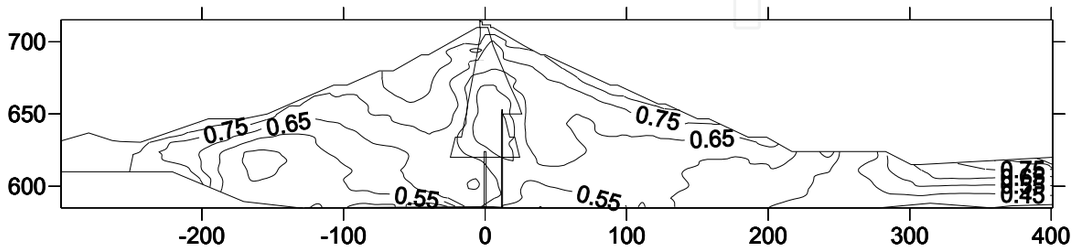

(d) stress level

Fig. 5. Stress distribution on section Y=210m

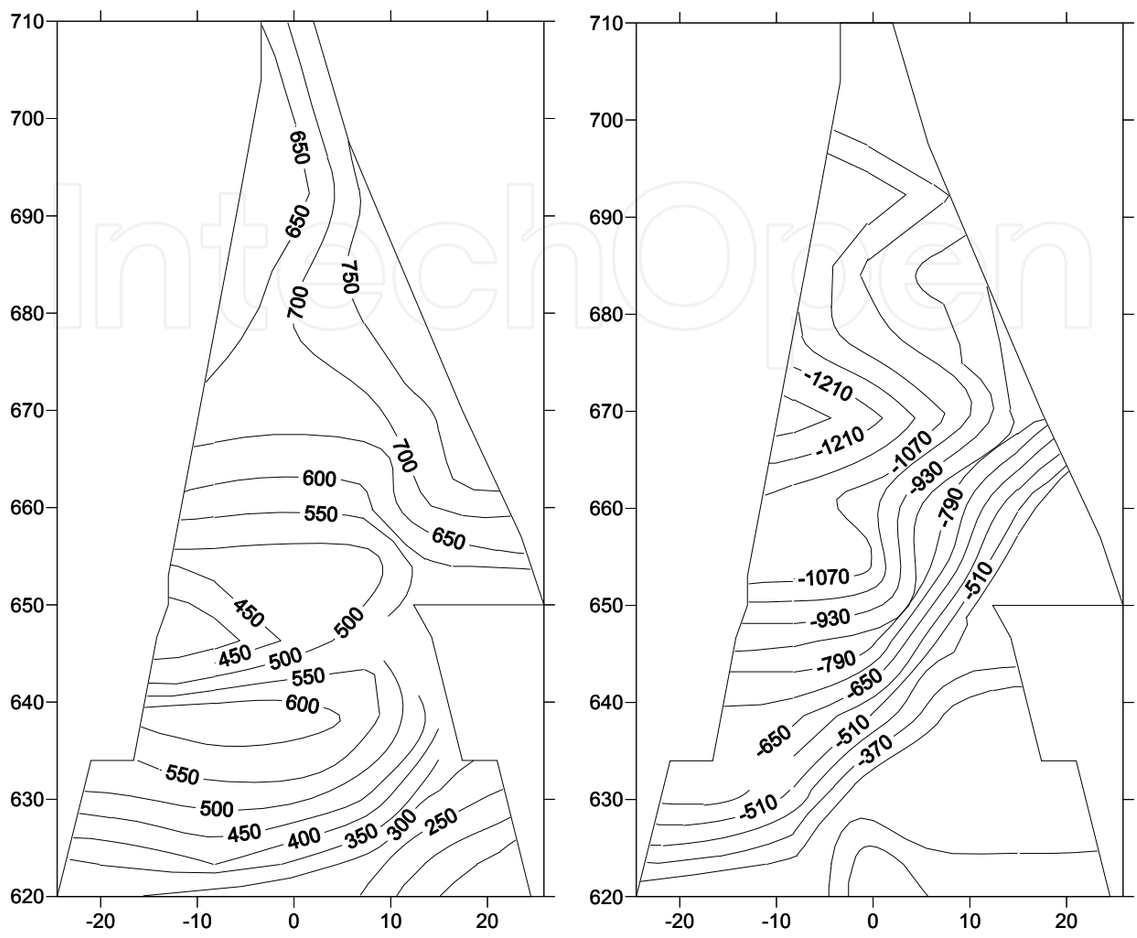

(a) X-displacement (b) Z-displacement

Fig. 6. Displacement distribution of core wall on section Y=210m (unit: mm)

3.2 Earthquake responses of dam

3.2.1 Finite element model

The finite element model what can be used to analyze earthquake responses of the dam is build, which is the same as the model for the static analysis.

3.2.2 Dynamic parameters and calculation condition

The time history analysis method is used and the equivalent nonlinear viscoelastic model is chosen as the constitutive model of soil, which assumes that the soil of dam body and foundation overburden are considered as viscoelasticity, and equivalent shear modulus G and equivalent damping ratio λ are applied to reflect the nonlinearity and hysteretic nature this two properties of soil dynamic stress-strain relation. The dynamic parameters of dam are shown as in Table 4 and Table 5.

Material parameters	Soil Material							
	loam	filter	rockfill	ballast	Gravel (dam)	Gravel (mud)	pebble	Gravel (foundation)
K	375	1875	2282	1147	2052	696	1701	1603
n	0.63	0.61	0.55	0.58	0.54	0.57	0.55	0.54

Table 4. Maximum dynamic shear modulus parameters of dam materials

Material parameters	Soil Material							
	loam	filter	rockfill	ballast	Gravel (dam)	Gravel (mud)	pebble	Gravel (foundation)
K_a	0.4653	1.5232	2.2814	1.6118	1.6653	1.4226	2.1450	1.6603
n_a	1.1883	1.2100	2.0871	1.5464	1.5553	1.2002	2.0322	1.4876
K_v	1.8252	2.0632	2.3221	1.7877	1.7623	1.5308	2.2895	1.7222
n_v	1.7119	1.9121	2.2007	1.6206	1.5989	1.3359	2.1659	1.5098

Table 5. Residual strain parameters of dam materials

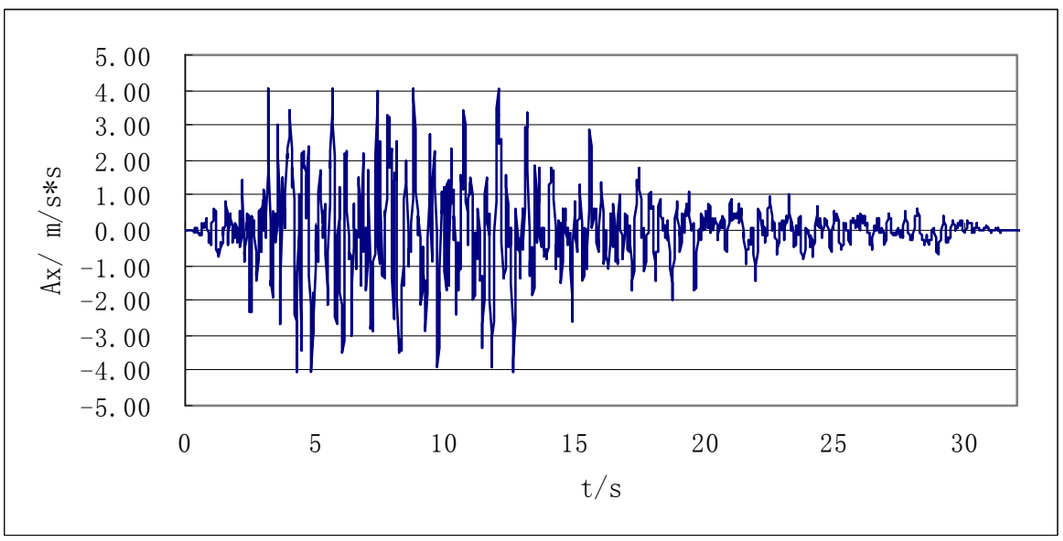

Fig. 7. The input curve of earthquake acceleration of bedrock in horizontal direction

Under the Wenchuan earthquake condition, in the dam site of Bikou hydropower station, the seismic intensity is comprehensively evaluated as degree 9. Correspondingly, the bedrock in the dam site has a peak level acceleration of 404cm/s^2 and its seismic acceleration curve of bedrock in horizontal direction is shown as Fig.7, which is in up-down stream direction and in dam axis direction. When calculating, the seismic acceleration value of vertical direction is regarded as two thirds of the horizontal one. Meanwhile, the dynamic water pressure is evaluated by the additional mass method called Westergaard method, that using equivalent additional mass instead of the dynamic water pressure to stack with the quality of the dam body during the earthquake.

3.2.3 Earthquake responses

Under the conditions of Wenchuan earthquake intensity, the earthquake response of the dam are analyzed, including the maximum acceleration response, displacement response and stress response of dam body, loam core and cut-off walls, and the earthquake induced permanent deformation (Serff et al., 1976; Taniguchi et al., 1983; Kuwano & Ishihara, 1988; Cascone & Rampello, 2003; Elia et al, 2011) of the dam is also obtained. The maximum values of earthquake responses analysis results are shown as in Table 8.The distributions of the dynamic analysis main features (Idriss et al., 19773; Ahmed-Waeil et al., 1990a, 1993b; Zhu et al., 2003) are shown as in Fig.8~Fig.14.

1. Acceleration response

Calculation results show that the natural vibration period of Bikou dam is about 0.74 seconds. The maximum acceleration response of the rockfill respectively is 4.08m/s^2 along the river direction, 4.43m/s^2 along the dam axis direction and 3.20m/s^2 along the elevation direction. For the core, the maximum acceleration response along the above three directions are 3.89m/s^2,4.14m/s^2 and 3.14m/s^2 respectively. Along the dam axis direction, the acceleration response of the dam is the greatest, followed by the acceleration response along the river direction and the acceleration response along the elevation direction is the smallest.

When earthquake comes, the upstream and downstream dam shell materials, which have a relatively long distance to the cut-off wall, are slightly affected. The corresponding horizontal acceleration response is basically proportional to the dam height and the maximum one appears near the upstream and the downstream slope surfaces which are close to the dam crest. The seismic acceleration response of a point is related to the vertical distance between the point and the bottom of the river valley; the height is greater, the corresponding seismic response is greater. As the slide slope of the right bank is slower than the left bank, the maximum horizontal acceleration response appears much closer to the right bank. From the middle of river bed to the both banks, the horizontal acceleration response decrease gradually which is related to the dam body type and boundary conditions. From the distribution of acceleration response on cross section, it can be seen that near the right bank, as the base of the downstream dam body is higher than the upstream and overburden layer exist at the bottom of the upstream dam body, the acceleration response of the upstream dam body is greater than the downstream dam body. The situation is opposite near the left bank, as deep overburden layer exists at the bottom of the downstream dam body and the downstream dam slope is much steeper than the upstream, the acceleration response of the downstream dam body is greater than the upstream dam body.

2. Displacement response

The maximum displacement response of the rock-fill is 25.92mm along the river direction, 16.99mm along the dam axis direction and 12.39mm along the elevation direction. For the loam core, the maximum acceleration response along the above three directions are 25.61mm, 16.77mm and 12.33mm respectively.

The displacement responses are not so great. Along the river direction, the displacement response of the dam is the greatest, followed by the displacement response along the dam axis direction. The smallest displacement response is along the elevation direction. The distribution of displacement response is almost the same with acceleration response. Under the seismic action, the displacement response is basically proportional to the dam height and the maximum one appears near the upstream and the downstream slope surfaces which are close to the dam crest. The seismic acceleration response of a point is related to the vertical distance between the point and the bottom of the river valley, the height is greater, corresponding seismic response is greater. The maximum horizontal displacement response appears near the dam crest above the deepest site of river valley. As overburden exists at the left bank, the maximum vertical displacement appears much closer to the left bank. From the center of river bed to the both banks, the displacement response decreases gradually which is related to the dam body type and boundary conditions. From the distribution of displacement response on cross section, the displacement response of the dam is not only related to the grade of upstream and downstream slope, but also the depth and distribution of overburden. Close to the right bank, as the base of the downstream dam body is higher than the upstream and overburden layer exists at the bottom of the upstream dam body, the displacement response of the upstream dam body is greater than the downstream dam body. The situation is opposite near the left bank. As deep overburden layer exists at the bottom of the downstream dam body and the downstream dam slope is much steeper than the upstream, the displacement response of the downstream dam body is greater than the upstream dam body.

3. Stress response

For the rockfill of dam, the maximum first principal stress is 425kPa, the maximum second principal stress is 352kPa and the maximum third principal stress is 203kPa. For the core, the maximum first principal stress is 265kPa, the dynamic tensile stress is 221kPa; the maximum second principal stress is 215kPa, the dynamic tensile stress is 178kPa; the maximum third principal stress is 192kPa, the dynamic tensile stress is 157kPa. For the first concrete cut-off wall, the maximum first principal stress is 3031kPa, the maximum second principal stress is compressive stress with a value of 591kPa and the maximum third principal stress is compressive stress with a value of 363kPa. For the second concrete cut-off wall, the maximum first principal stress is 4482kPa, the maximum second principal stress is compressive stress with a value of 683kPa and the maximum third principal stress is compressive stress with a value of 422kPa.

The stress response of rockfill and core along the river direction is the greatest, followed by the displacement response along the dam axis direction and the displacement response along the elevation direction is the smallest. The strong stress response of the core happens on the major river bed where the loam core connects to the both banks. The big and small principal stress response of the rock-fill become stronger with the increase of cover depth,

thus the contour lines are parallel to the dam slope, and the maximum dynamic compressive stress and maximum dynamic tensile stress appear at the bottom of the dam near the deepest river valley. At the same elevation, the stress response of the dam body is much stronger than the core. As the great difference of deformation modulus between concrete and loam, stress concentration appears near the cut-off wall. Besides, at the downstream side of cut-off wall, dynamic stress response is very strong. From the distribution of stress response on longitudinal profile, it can be seen that the stress response at the bottom of the dam on the right bank is a bit stronger than on the left bank, the dynamic stress response is great at the connecting part between dam body and both bank slopes, especially near the place where the section of bank slope varies, stress concentration of strong dynamic stress response appears; and with the increase of peak acceleration, the stress response becomes stronger. So, more attentions should be paid to these weak areas.

Great dynamic stress appears at the top of the concrete cut-off wall, so does in the connection part between bedrock and the cut-off wall close to the bank slope. The stress response of concrete is proportional to the peak seismic acceleration, thus with the increase of peak acceleration, the dynamic tensile stress and compressive stress become greater. The maximum dynamic tensile stress of the cut-off wall is shown as in Table 6. Overall, the dynamic compressive stress of concrete is small and the dynamic tensile stress is relatively much greater, so the monitoring to the strength of the cut-off wall should be strengthened to ensure the safety operation of the dam.

During the earthquake, the maximum shear stresses of the dam are respectively 236kPa. On the cross section of the dam, the maximum dynamic shear stress and the dynamic shear stress become greater gradually from the upstream side and downstream side to the dam axis; but in the middle of the core, the dynamic shear stress decreases greatly, and at the bottom of dam, the dynamic shear stress response of rock-fill and transition material are very great. So, as the significant difference of the filling materials, the maximum shear stress responses are very significant in the connection parts of materials. The shear stress response of rock-fill is very great on the bank slope where the sections vary, and shear stress concentration appears in the local areas of where the sections vary at both banks; in the main river bed where the core connects to both bank, the shear stress is great.

4. Earthquake induced permanent deformation

The maximum permanent horizontal displacement is 74mm along the river direction, 47mm along the dam axis direction and the maximum permanent vertical displacement or settlement is 239mm. Taking no account of the thickness of the overburden on the dam foundation, the maximum dam height is 101.8m, then the permanent settlement induced by earthquake is about 0.23 percents of the dam height.

Due to the upstream water pressure, the earthquake induced permanent deformation of the core along the river orientation points to the downstream, so does the upstream dam shell materials near the dam crest. Along the dam axis direction, the earthquake induced permanent deformation is not so great and the maximum one appears near the upstream dam slope. It can be seen that in the dam abutments of both banks, the displacements of the dam body point to the center of the river valley; near the dam axis, the displacement and its variation gradient at the right bank are greater than the left bank. Affected by the concrete

Item			Value
maximum absolute acceleration response / m·s^{-2}	Rockfill	up-down stream direction	4.08
		dam axis direction	4.43
		vertical direction	3.20
	Core wall	up-down stream direction	3.89
		dam axis direction	4.14
		vertical direction	3.14
maximum displacement response /mm	Rockfill	up-down stream direction	25.92
		dam axis direction	16.99
		vertical direction	12.39
	Core wall	up-down stream direction	25.61
		dam axis direction	16.77
		vertical direction	12.23
maximum stress response of rockfill /kPa	Rockfill	1st principal stress	425/-422
		2nd principal stress	352/-347
		3rd principal stress	203/-188
	Core wall	1st principal stress	265/-221
		2nd principal stress	215/-178
		3rd principal stress	192/-157
	1st cut-off wall	1st principal stress	3031/-2908
		2nd principal stress	591/-589
		3rd principal stress	363/-316
	2nd cut-off wall	1st principal stress	4482/-3759
		2nd principal stress	683/-665
		3rd principal stress	422/-387
Earthquake induced permanent deformation/mm		stream direction (up/down stream)	74/-49
		dam axis direction (left /right bank)	47/-26
		vertical direction(settlement)	-239
maximum shear stress response / kPa			236

Table 6. Earthquake responses of Bikou dam by 3-D dynamic FEM

cut-off wall, the ultimate settlement of dam body below the elevation of 650m is small. And the settlement of the dam body above the river valley is basically uniform from the right side to the left, and the permanent deformation increases with the elevation increases. The maximum settlement appears near the downstream dam crest which is close to the dam axis. In general, the earthquake induced permanent deformations in both conditions are not great.

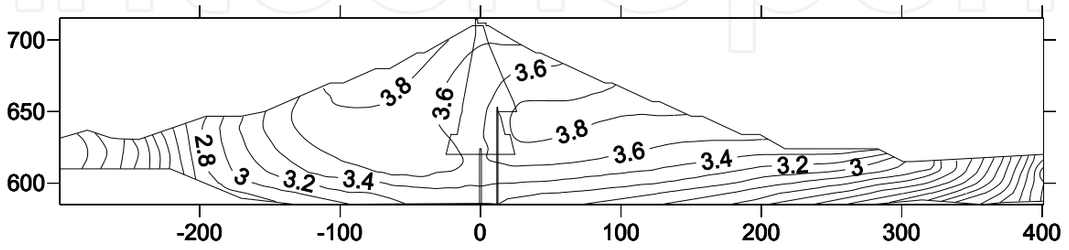

(a) X-direction (section Y=210m)

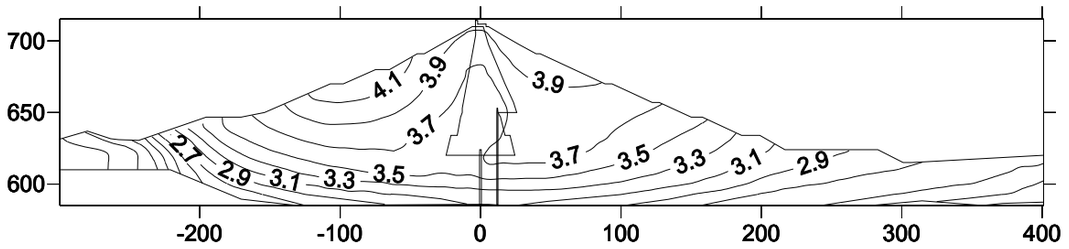

(b) Y-direction (section Y=210m)

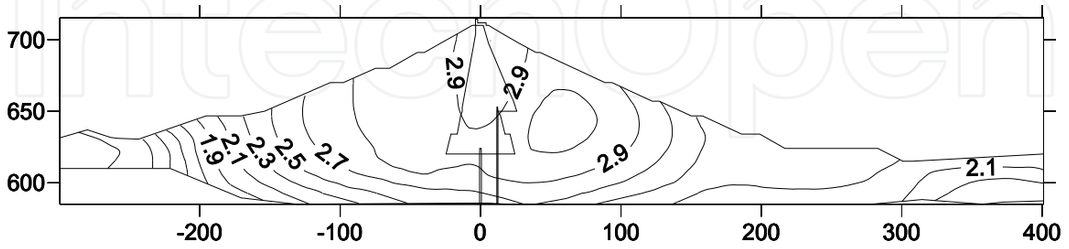

(c) Z-direction (section Y=210m)

Fig. 8. Distribution of maximum absolute acceleration response (m/s^{-2})

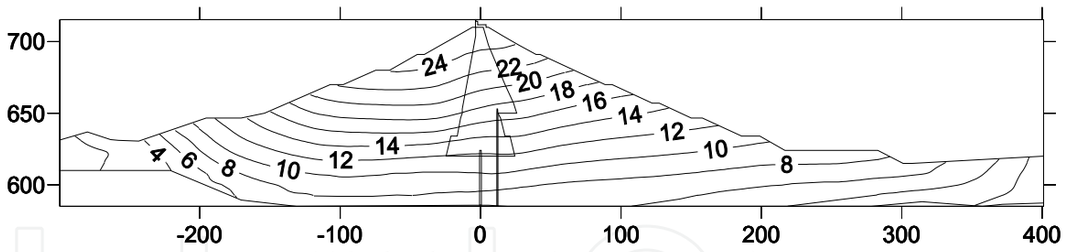

(a) X-displacement (section Y=210m)

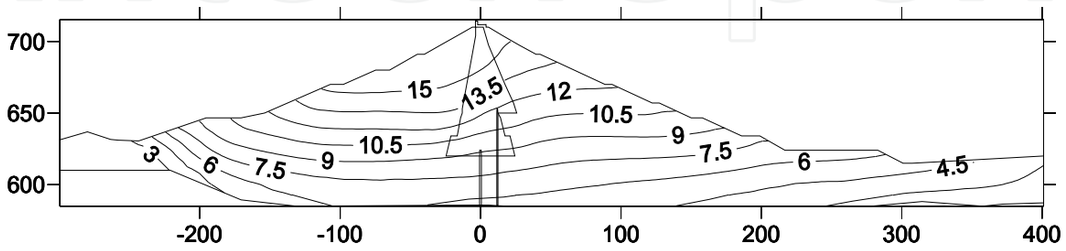

(b) Y-displacement (section Y=210m)

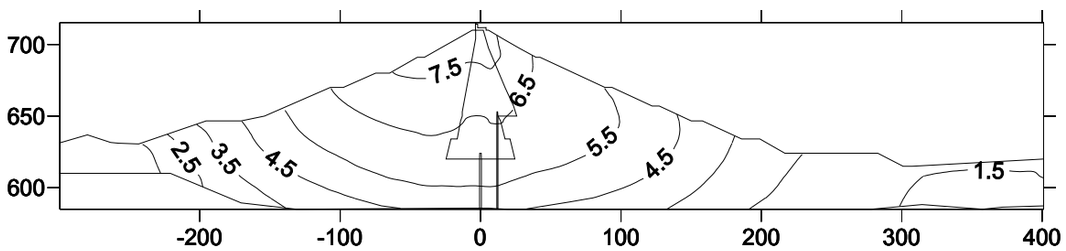

(c) Z-displacement (section Y=210m)

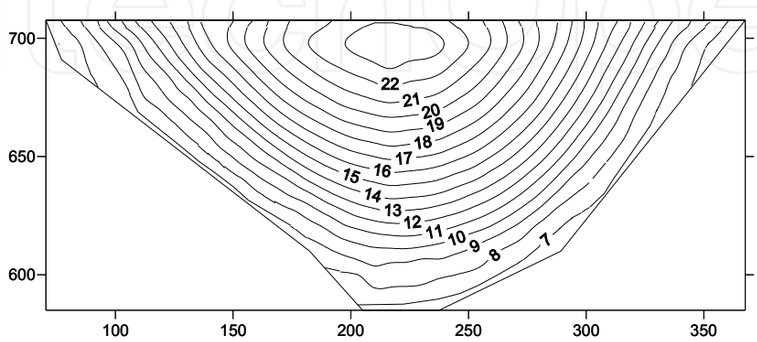

(d) X-displacement (section X=-10m)

Fig. 9. Distribution of maximum displacement response (mm)

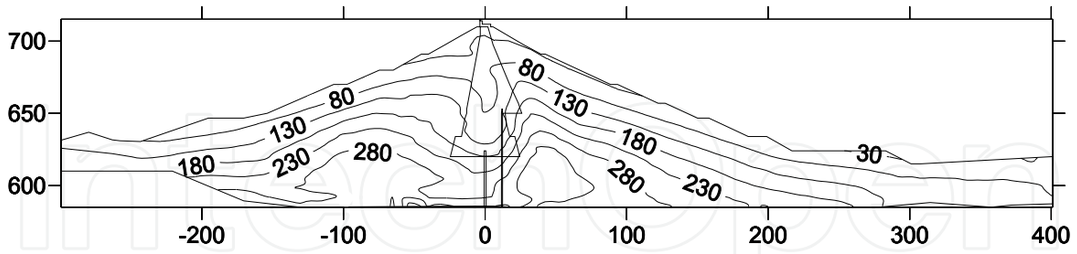

(a) the first principal stress

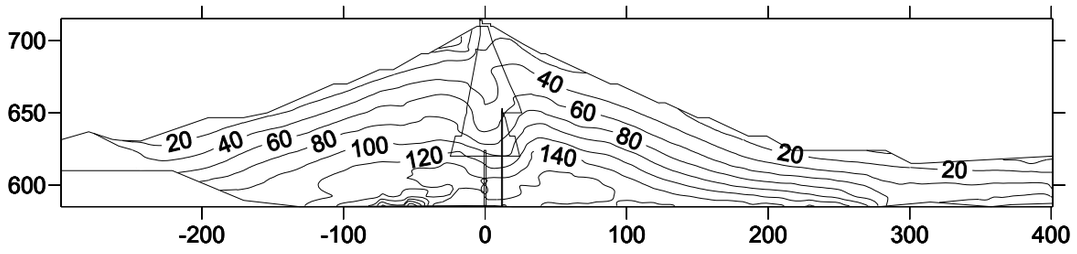

(b) the second principal stress

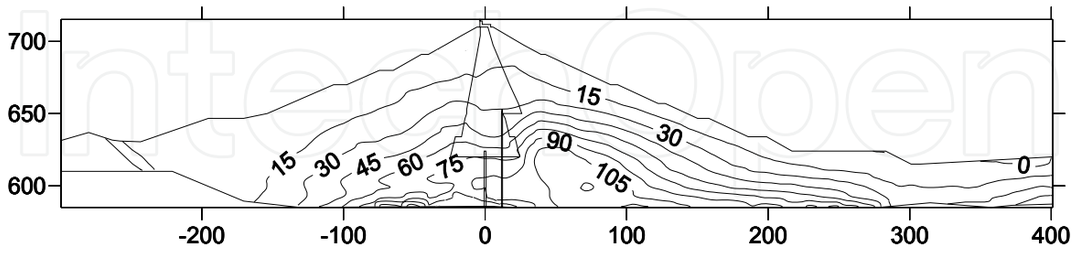

(c) the third principal stress

Fig. 10. Distribution of maximum stress response on section (Y=210m) (unit: kPa)

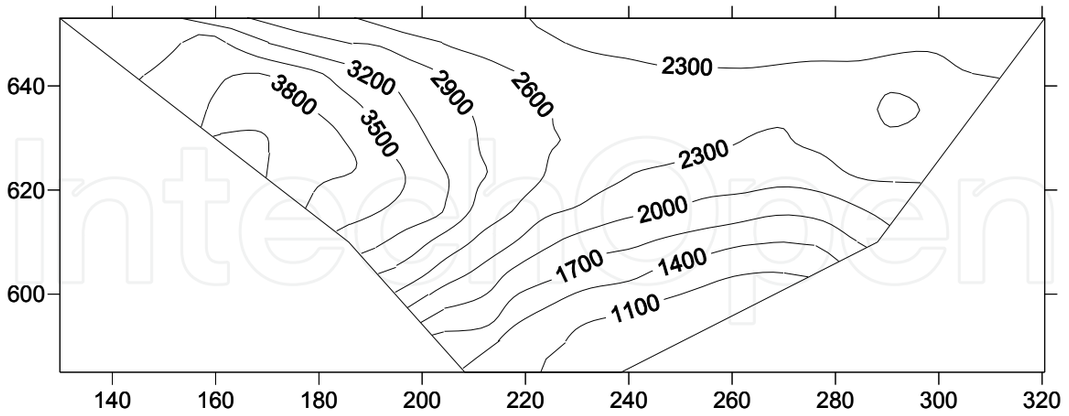

(a) the first principal stress

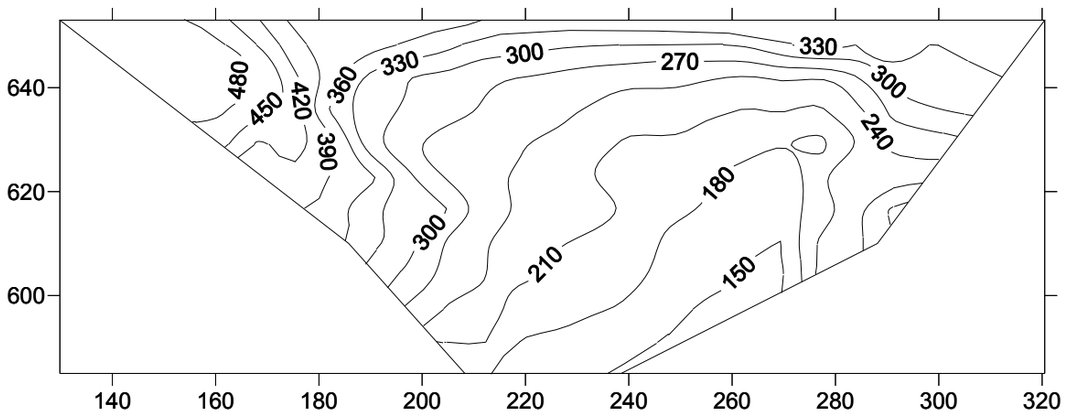

(b) the second principal stress

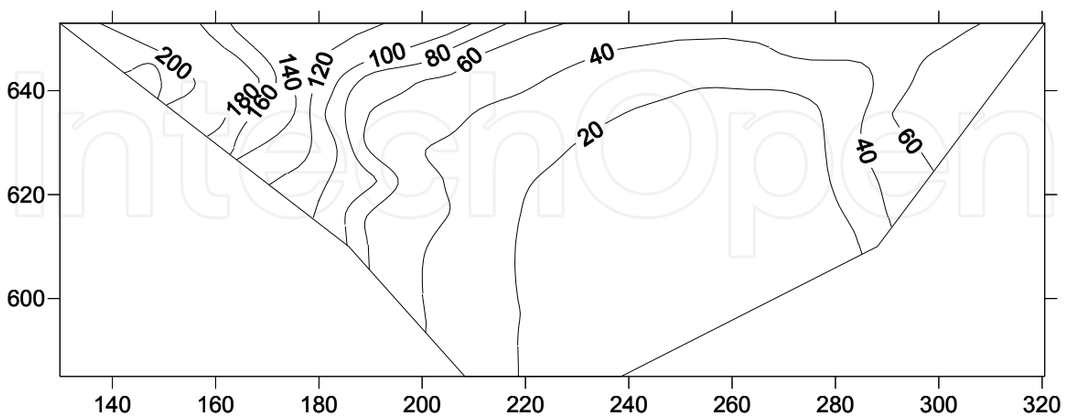

(c) the third principal stress

Fig. 11. Distribution of maximum stress response of the second cut-off wall (unit: kPa)

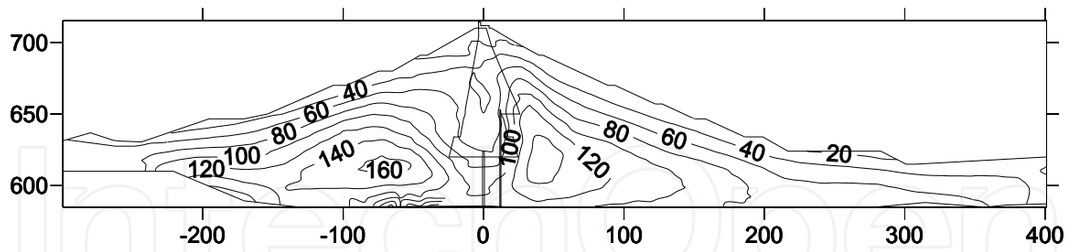

Fig. 12. Distribution of maximum dynamic shear on section (Y=210m) (unit: kPa)

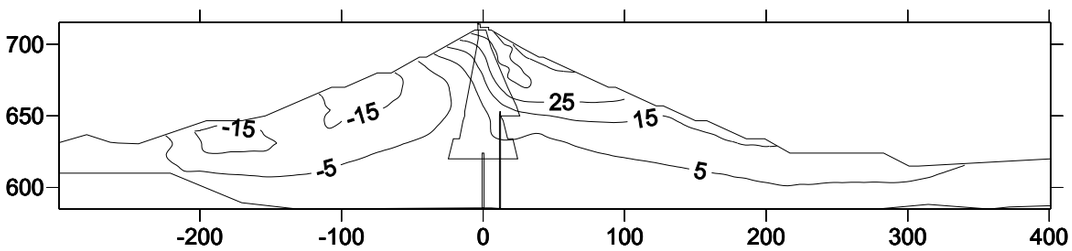

(a) X-direction

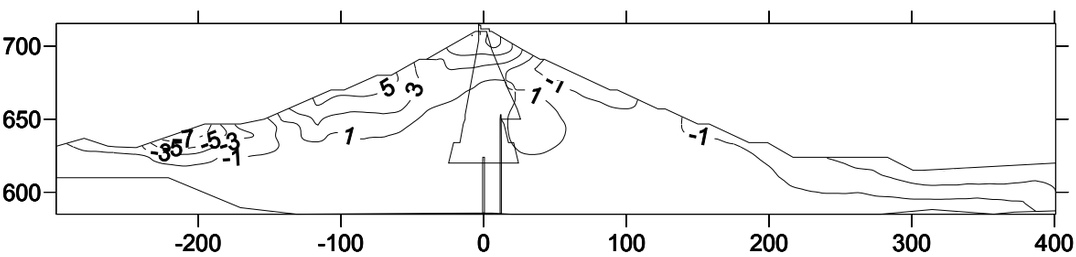

(b) Y-direction

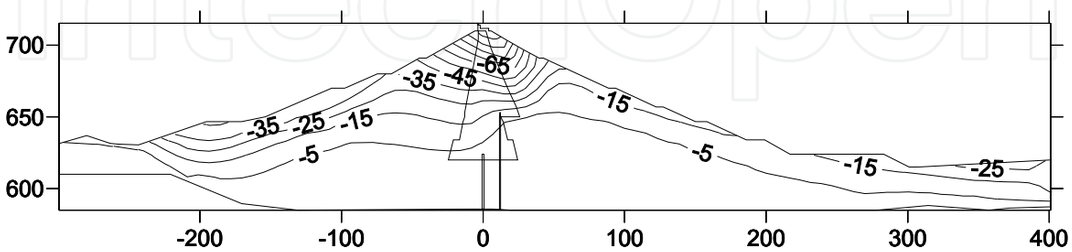

(c) Z-direction

Fig. 13. Distribution of earthquake induced permanent deformation on section(Y=210m) (mm)

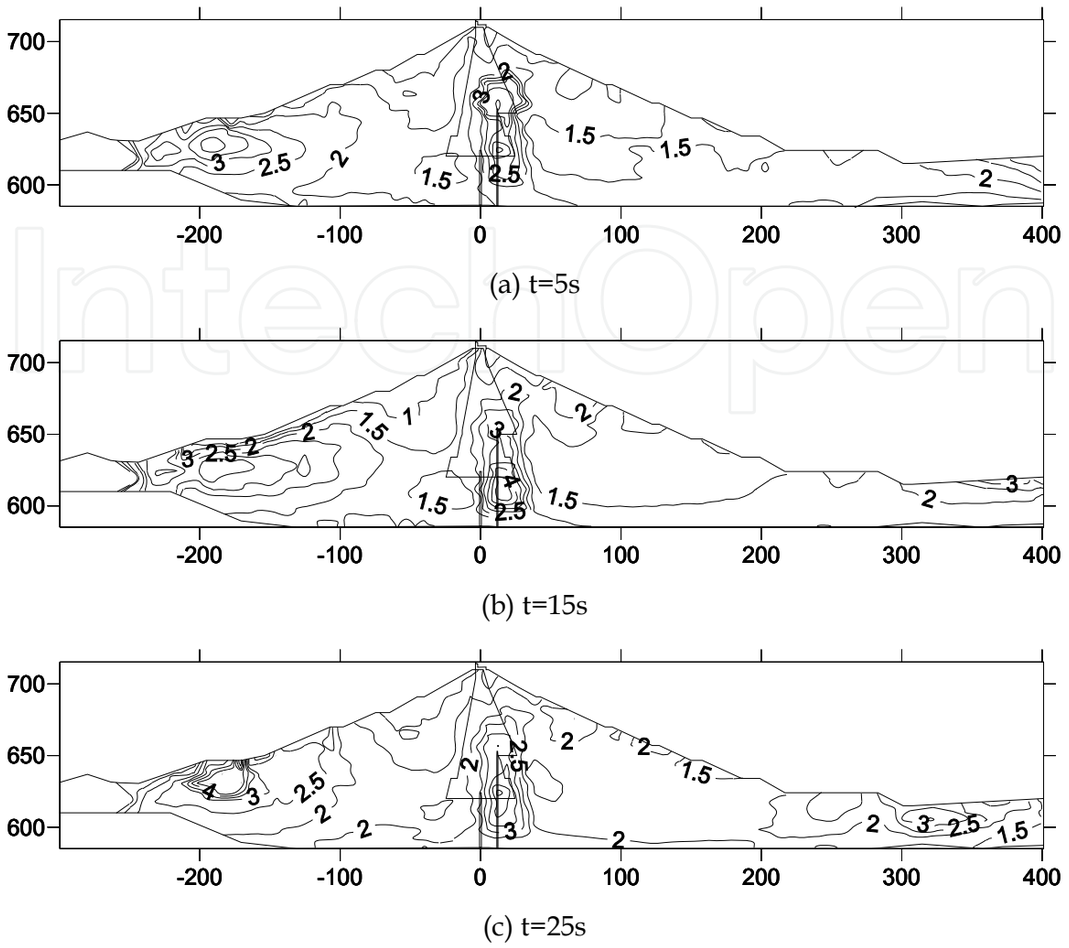

Fig. 14. Distribution of safety factors at different times during earthquake on section (Y=210m)

4. Earthquake-resistance safety evaluation

4.1 Comparing the static calculation results and monitoring data

In order to monitor the consolidation settlement in construction and operation, 5 collimating lines are set for the Bikou Hydropower Station soil core dam(Fig.18), which are respectively up dam 0-010.1m(708.00m elevation), under dam 0+007.8m(709m elevation), under dam 0+041.8m(691m elevation), under dam 0+093.0(670m elevation) and under dam 0+142.7(650m elevation). Only up dam section 0-010.0m got observed on December 17, 1975, and other sections started observation two years later after storage for the construction of crest parapet wall and downstream slope and drainage. Monitoring date of dam surface horizontal displacement and settlement before earthquake are shown as in Fig.16 and Fig.17.

Among all the monitoring sites, only section 0-010.0m started observation once storage, while other sections started observation relatively late. Therefore, displacement of these 5 sections cannot directly be compared with that of finite element calculation. As section 0-

010.0m got monitored earlier, its monitoring date should be compared with modified results of finite element calculation, which can be shown as in Fig.16 and Fig.17.

According to the settlement distribution (Fig.18) along dam axis direction of section 0-010.0m, settlements of monitoring points on crest are approximately proportional to their corresponding rock-fill thickness at the same place. Crest position where locates on the deepest valley floor has the biggest settlement, and settlement on right bank is larger than that on left bank. Settlement distribution discipline of finite element calculation is roughly the same with that of monitoring results. Additionally, calculation values are larger than monitoring data, since dam settlement started monitoring later than corresponding calculation situation, then displacement before monitoring was included in the calculation results.

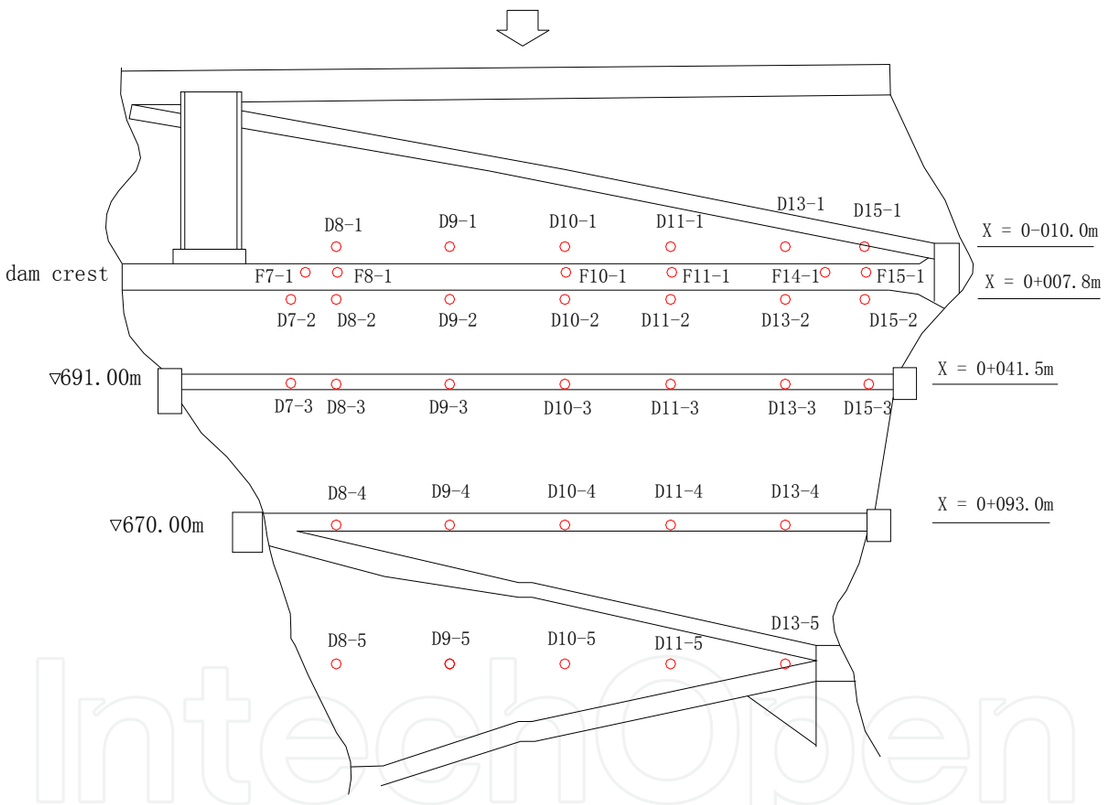

Fig. 15. Layout of monitoring point

Considering the starting observation time of section 0-010.0m, settlements of monitoring points are values after reservoir started storage. Thus, calculation results of finite element analysis should include the settlement values when dam body filling had been finished, that is, settlements incremental in the operation and completion periods. The calculation values are smaller than values of monitoring. It's because that calculation model only considers principal deformation and ignores the rheological of dam body. From the comparison of crest settlement above, calculation model and parameters are reasonable and fundamentally match the reality.

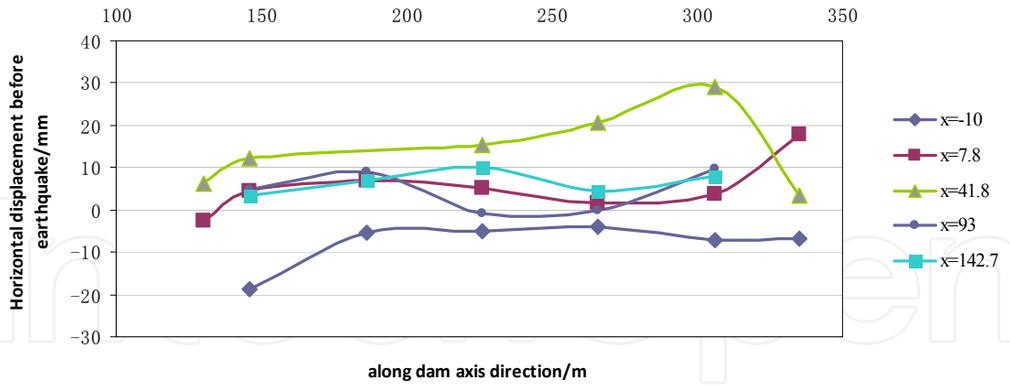

Fig. 16. Distribution of horizontal displacement measured value before the earthquake

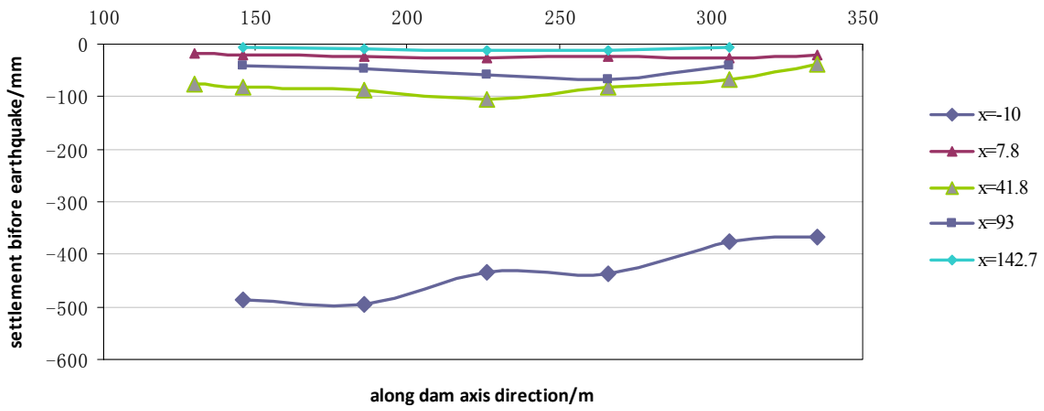

Fig. 17. Distribution of settlement measured value before the earthquake

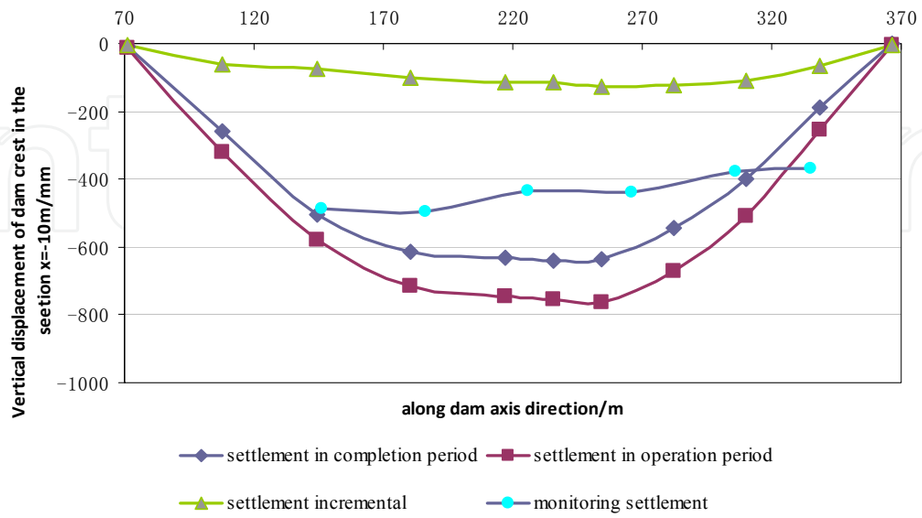

Fig. 18. Comparison of the settlement measured value and calculated value before the earthquake on the section (X=-10.0m)

4.2 Results of earthquake-resistance analysis

In the process of dynamic calculation, safety factor development of every element, excluding bed rock, concrete cut-off walls, wave wall and joints, has been completely recorded throughout earthquake. The safety factor is defined as the ratio of shear strength to shear stress (including both static and dynamic shear stress) of element potential failure surface. As it to analyze the seismic safety of upstream and downstream, the anti-slide stability coefficient is calculated on pseudo-static method. Sweden Slice Method is adopted for slope stability analysis, where both horizontal and vertical seismic actions are considered.

Calculation condition for slope anti-slide stability can be seen in Table 7. The smallest safety factors of upstream and downstream slopes are shown as in Table 8, and the potential sliding surfaces are shown as in Fig.19. As the compacted earth dam design specification (SL274-2001) says that the smallest anti-slide stability factor under seismic action should be no less than 1.15. Under the condition BK-S1, slope stability of Bikou dam cannot meet the present criterion. However, on the conclusion of Bikou station injuring survey under "5.12" Wenchuan earthquake and its initial analysis report, only some joints connecting crest and body to embankment were damaged and needed amending, yet the whole dam was safe in general. Under the seismic action, safety factor of Bikou dam does not satisfy demand, however, the dam did not suffer from sliding or slope instability during the "5.12" Wenchuan earthquake. So, it is suggested that smaller safety factors should be adopted. For example, a level 2 dam has a safety factor ranging from 1.05 to 1.10. In a word, the safety factor distribution suggests that the Bikou dam has some partial scopes where the factors are less than 1 near the crest and upstream and downstream slopes. But the scales are sporadic and will not lead the failure of dam slopes.

Condition	Dam slope	Peak acceleration /g	Upstream water level/m	Downstream water level/m
BK-S1	Upstream and downstream	0.404	707.00	617.02

Table 7. Condition for dam stability analysis

Condition	Peak acceleration/g	Dam slope	Fs
BK-S1	0.404	upstream	1.11
		downstream	1.19

Table 8. Results for dam stability analysis

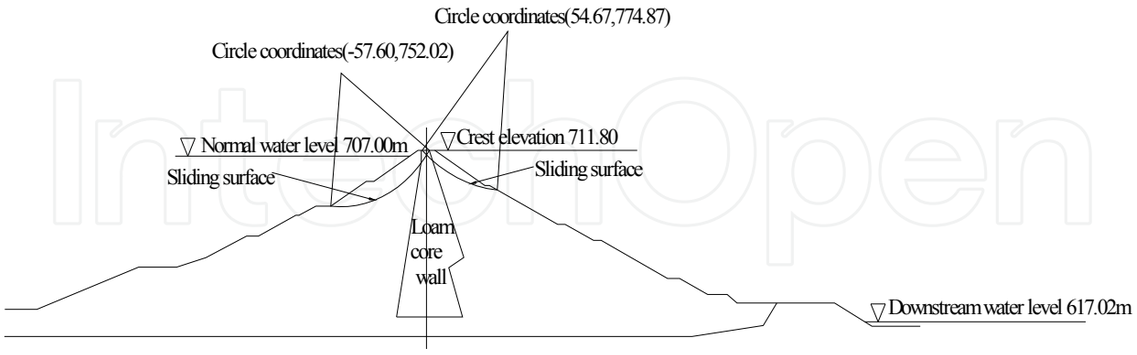

Fig. 19. Dangerous sliding surface position schemes of dam slopes (condition BK-S1)

5. Conclusions

In this paper, according to the actual engineering conditions of Bikou earth core rockfill dam, the 3-D non-linear FEM model of the dam is set up for calculating earthquake response by the dynamic time-history analysis method. By simulating the process of the filling of dam body and reservoir impounding, firstly the original static stress field of dam body is obtained under the normal water level. Then by the dynamic time-history analysis method, the earthquake responses of the dam, including acceleration response, displacement response, stress response and the earthquake induced permanent deformation of the dam are obtained for inputting the earthquake with peak acceleration of bedrock 404cm/s^2. Under the action of the seismic with peak acceleration 404cm/s^2, the acceleration response along the up-downstream direction is maximal with the value of 4.08m/s^2, the one along the dam axis is secondary with the value of 4.43m/s^2, and the one along vertical direction is the minimum with the value of 3.20m/s^2. The maximum displacement response of dam in the three directions are 25.92mm, 16.99mm, and 12.39mm respectively, and the maximum principle stress responses of rockfill body are 425kPa, 352kPa, and 203kPa respectively. The maximum earthquake induced permanent settlement is 239mm, about 0.23 percents of the dam height. It is shown that the earthquake responses of the dam are close to the recorded data. The theories and methods for analyzing the earthquake responses of the earth dam here are feasible, and the results are consistence with the real situation of post-earthquake.

6. Acknowledgement

This paper was supported by the Key Project of National Natural Science Foundation of China (Grant NO. 40930635) and Non-profit Projects Research of Ministry of Water Resources of China (Grant NO. 200901070). Grant NO 2009586012, entitled “State Key

Laboratory of Hydrology-Water Resources and Hydraulic Engineering" provided partial support for this work.

7. References

Ahmed-Waeil, M. E., & Ramana, V. G. (1993). Dynamic behaviour and seismic response of El Infiernillo dam. *Earthquake Engineering & Structural Dynamics*, 1993, Volume 22 Issue 8, pp. 665-684

Ahmed-Waeil, M. E., Ronald, F. S., Mohamed, F. S., et al. (1990). La Villita Dam Response During Five Earthquakes Including Permanent Deformation. *Journal of Geotechnical Engineering (ASCE)*, Vol.116, No.10, October 1990, pp. 1443-1462

Cao, Z. Z., Youd, T. L., and Yuan X. M. (2011). Gravelly soils that liquefied during 2008 Wenchuan, China earthquake, Ms=8.0, *Soil Dynamics and Earthquake Engineering*, 2011, Vol. 31, pp.1132-1143.

Cascone, E., & Rampello, S. (2003). Decoupled seismic analysis of an earth dam, *SOIL DYNAMICS AND EARTHQUAKE ENGINEERING*, 2003, Vol. 23, pp.349-365

Chen, H. Q., Xu, Z. P., and Lee, M. (2008). Wenchuan Earthquake and seismic safety of large dams, *Journal of Hydraulic Engineering*, 2008, Vol.39, No.10, pp.1158-1167

Chen, L. Y., & Talwani, P. (1998). Reservoir-induced seismicity in China, *PURE AND APPLIED GEOPHYSICS*, 1998, Vol. 153, No. 1, pp.133-149

Duncan, J. M., and Chang, C. Y. (1970). Nonlinear analysis of stress and strain in soil, *Journal of the Soil Mechanics and Foundation Divisio*n, *ASCE*, 96(SM5), pp.l629-l653

Elia, G., Amorosi, A., Chan A, H. C., et al. (2011). Fully coupled dynamic analysis of an earth dam, *GEOTECHNIQUE*, 2011, Vol.61, pp.549-563

Gu, G. C. (1989). *Earthquake Engineering for Earth-rock Dams*, Hohai University Press, Nanjing , 1989

Hardin, B. O., & Denevich, V. P. (1972). Shear moduls and damping in soil: design equations and curves. *ASCE*, 98 (SM7), pp.667-92

Hardin, B. O., & Denevich, V. P. (1972). Shear modulus and damping in soil: measurements and parameter effects. *ASCE*, 98 (SM6), pp.603-624

Idriss, I. M., Lysmer, J., Huang, R., et al. (1973), A computer program for evaluating the seismic response of soil structures by variable damping finite element procedures, Berkeley, College of Engineering University of California.

Kenneth, G. (2011). Dermatology Aboard the USNS COMFORT: Disaster Relief Operations in Haiti After the 2010 Earthquake, *Dermatologic Clinics*, 2011, Vol. 29, No.1, pp.15-19

Kuwano, J., & Ishihara, K. (1988). Analysis of permanent deformation of earth dams due to earthquake, *Soils and Foundations*, Vol, 28(01), pp.41-55

Lin, P., Wang, R. K., and Li, Q. B. (2009). Effect Analysis of Structural Safety of Typical Large Dams in Wenchuan 8.0 Earthquake, *Chinese Journal of Rock Mechanics and Engineering*, 2009,Vol.28, No.6, pp. 1261~1268

Mejia, L. H. (1981). Three dimensional dynamic response analysis of earth dam, *Report No. UCB/EERC-81/15*. Berkeley, University of California

Mejia, L. H., Seed, H. B., & Lysmer, J. (1982). Dynamic analysis of earth dams in three dimensions, *Journal Geotechnical Engineering Division (ASCE)*, 1982, 108(GT12), pp. 1354-1376

Pan, R. Y. (2009). *Analysis of the recheck of the earthquake damage of Bikou Core Rockfill Dam*, Hohai University, Nanjing,2009

Pei, S. P., Su, J. R., Zhang, H. J., et al. (2010). Three-dimensional seismic velocity structure across the 2008 Wenchuan M_s 8.0 earthquake, Sichuan, China, *Tectonophysics*, 2010, Vol.491, pp.211-217

Serff, N., Seed, H. B., Makdisi, F. I., & Chang, C. K. (1976). Earthquake induced deformations of earth dams, *Report No. EERC/76-4*, Earthquake Engineering Research Center, University of California, Berkely, 1976

Shen, Z. Z., Wen, X.Y., and Lv, S.X. (2006). Analysis of earthquake responses for Jiudianxia concrete face rockfill dam, L. Berga et al eds, *Dams and Reservoirs, Societies and Environment in the 21st Century*, Published by Taylor & Francis/Balkema, London, 2006, Vol. 1, pp.925–930

Shen, Z. Z., Xu, L.Q., and Wang, W. (2010). Earthquake response of Xika concrete face rockfill dam by EFM, *Engineering, Science, Construction, and Operations in Challenging Environments, 2010 ASCE*, pp.463-472

Takewaki, I., Murakami, S., Fujita, K., et al. (2011). The 2011 off the Pacific coast of Tohoku earthquake and response of high-rise buildings under long-period ground motions, *Soil Dynamics and Earthquake Engineering*, 2011, (In press)

Talwani, P. (1997). On the nature of reservoir-induced seismicity, *PURE AND APPLIED* GEOPHYSICS, 1997, Vol. 150, pp.473-492

Taniguchi,E., Whiteman, R.V., & Warr, W. A. (1983). Prediction of earthquake induced deformation of earth dams, *Soils and Foundations*, 1983, Vol. 23(4)

Wang, W. X., Sun, W. K., and Jiang, Z. S. (2010). Comparison of fault models of the 2008 Wenchuan earthquake (M_s8.0) and spatial distributions of co-seismic deformations, *Tectonophysics*, 2010, Vol.491, pp.85-95

Xenaki, V. C., & Athanasopoulos, G. A. (2008). Dynamic properties and liquefaction resistance of two soil materials in an earthfill dam - Laboratory test results, *SOIL DYNAMICS AND EARTHQUAKE ENGINEERING*, 2008, Vol. 28, pp. 605-620

Yu, H. Y., Wang, D., Yang, Y.Q., et al. (2009). The preliminary analysis of strong ground motion records from the M_s 8.0 Wenchuan Earthquake. *Journal of Earthquake Engineering and Engineering Vibration*, 2009, Vol.29, No.1, pp.1~13

Zeghal, M., & Abdel-Ghaffar, A. M. (2009). Evaluation of the Nonlinear Seismic Response of an Earth Dam: Nonparametric System Identification, *JOURNAL OF EARTHQUAKE ENGINEERING*, 2009, Vol.2009. pp. 384-405

Zhou, J. P., Yang, Z. Y., Fan, J. X., et al. (2009). Seismic Damage Investigation on Large and Medium Sized Hydropower Projects in Wenchuan Earthquake Area. *Chinese Journal of Water Power*, 2009,Vol.35,No.5, pp.1-6

Zhu, S., Wen, S.Q., and Huang, Y. M. (2003). Deformation and Stress Calculation for A 200m High CFRD, *Journal of Hohai University (Natural Sciences)* ,2003, 31(6):631-634

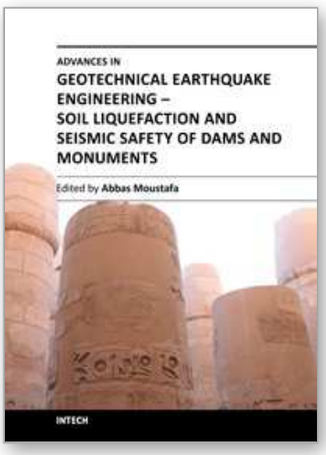

Advances in Geotechnical Earthquake Engineering - Soil Liquefaction and Seismic Safety of Dams and Monuments

Edited by Prof. Abbas Moustafa

ISBN 978-953-51-0025-6
Hard cover, 424 pages
Publisher InTech
Published online 10, February, 2012
Published in print edition February, 2012

This book sheds lights on recent advances in Geotechnical Earthquake Engineering with special emphasis on soil liquefaction, soil-structure interaction, seismic safety of dams and underground monuments, mitigation strategies against landslide and fire whirlwind resulting from earthquakes and vibration of a layered rotating plant and Bryan's effect. The book contains sixteen chapters covering several interesting research topics written by researchers and experts from several countries. The research reported in this book is useful to graduate students and researchers working in the fields of structural and earthquake engineering. The book will also be of considerable help to civil engineers working on construction and repair of engineering structures, such as buildings, roads, dams and monuments.

How to reference

In order to correctly reference this scholarly work, feel free to copy and paste the following:

Zhenzhong Shen, Lei Gan, Juan Cui and Liqun Xu (2012). Earthquake Response Analysis and Evaluation for Earth-Rock Dams, Advances in Geotechnical Earthquake Engineering - Soil Liquefaction and Seismic Safety of Dams and Monuments, Prof. Abbas Moustafa (Ed.), ISBN: 978-953-51-0025-6, InTech, Available from: http://www.intechopen.com/books/advances-in-geotechnical-earthquake-engineering-soil-liquefaction-and-seismic-safety-of-dams-and-monuments/earthquake-response-analysis-and-safety-evaluation-for-earth-rock-dams

INTECH
open science | open minds

InTech Europe
University Campus STeP Ri
Slavka Krautzeka 83/A
51000 Rijeka, Croatia
Phone: +385 (51) 770 447
Fax: +385 (51) 686 166
www.intechopen.com

InTech China
Unit 405, Office Block, Hotel Equatorial Shanghai
No.65, Yan An Road (West), Shanghai, 200040, China
中国上海市延安西路65号上海国际贵都大饭店办公楼405单元
Phone: +86-21-62489820
Fax: +86-21-62489821

IntechOpen